



Quantification of seismic performance factors of the buildings consisting of disposable knee bracing frames



Elnaz Nobahar^a, Mojtaba Farahi^b, Massood Mofid^{c,*}

^a Department of Civil Engineering, Sharif University of Technology, Tehran, Iran

^b Department of Civil Engineering, Monash University, Melbourne, VIC 3800, Australia

^c Department of Civil Engineering, Sharif University of Technology, Tehran, Iran

ARTICLE INFO

Article history:

Received 29 January 2015

Received in revised form 11 May 2016

Accepted 12 May 2016

Available online 6 June 2016

Keywords:

Over-strength factor

Ductility factor

Disposable knee bracing

Incremental dynamic analysis

Response modification factor

ABSTRACT

Braced frames are prevalently utilized as lateral load resisting systems in common engineering practice. disposable knee bracing (DKB) frames are categorized as one of the well-known types of these frames. In such systems, braces provide stiffness, while the link elements play an important role as an energy-absorbing fuse. During an extreme loading, link members help the structure to dissipate the imposed energy by plastic deformations. In this research, bracing frames took advantage of shear and/or flexural link elements. The previous experimental results revealed that hysteresis behavior of link elements remains constant until a specific rotation. Hence, employing such links as parts of a lateral load resisting system can increase the energy absorption capacity of the system. However, designing structures with DKB frames based on common design guidelines demands for evaluating required design factors for these braced frames. Seismic performance factors such as response modification factor (R), over strength factor (Ω), Deflection amplification factor (C_d) and Ductility factor (μ_r) are required first to design any structural system. In order to quantify these factors for the intended braced frames, the procedure introduced in FEMA P695 was used in this research. Numerous archetype frames were designed based on assumed performance factors. The behavior of archetype frames were then examined through performing push-over and incremental dynamic analyses. Some indexes such as the collapse margin ratio and the adjusted collapse margin ratio were defined and calculated for the archetype frames based on the nonlinear analyses results. The values of the calculated indexes were eventually compared with the accepted values proposed by FEMA P695 to validate the presumed seismic performance factors of DKB systems.

© 2016 Published by Elsevier Ltd.

1. Introduction

The design of steel structures for earthquake loading must satisfy two important requirements. Sufficient stiffness and enough strength should be provided for any intended structure in the purpose that the story drifts would be reduced. The reductions in the drift of the stories prevent non-structural elements from damage. On the other hand, the designed structure should be ductile enough to undergo severe displacements while it still remains capable of sustaining gravity loads. The ductile behavior helps a structure to dissipate the imposed energy under severe loading such as ground motions [1,2]. Moment resisting frames can provide the required ductility for a building. On the other hand, employing eccentric braced frames as the lateral load resisting system of a building mitigates the lateral displacements and drifts due to the high lateral stiffness of braced frames. Therefore, the two mentioned lateral load resisting systems can be combined to reach a system with the optimum performance under severe seismic loading. Eccentric braced frames were initially introduced by Roeder and Popov [3–5]. Two

essential criteria for link members can be satisfied by selecting optimum eccentricity in the frames: 1) providing sufficient stiffness, 2) providing ductility based on shear and flexure behavior [6,7]. Moreover, link elements can be repaired or replaced simply after severe damages, which is another benefit of implementing the intended lateral load resisting system.

The disposable knee bracing (DKB) system has been recently developed by Aristizabal [8]. In this framing system, diagonal braces are connected to knee elements. The knee elements act as ductile fuses in a structure. Tolerating large plastic flexural and/or shear deformations, these elements help the whole structure to damp the input energy during a severe earthquake. In addition, the diagonal braces of a DKB frame provide adequate lateral stiffness. The most prominent deficiency of braced frames is the buckling of the diagonal braces. The inelastic deformation of the buckled braces can result in lateral instability and sudden reduction in the load bearing capacity of the braced frames. However, this problem is more mitigated in DKB systems because the knee elements play the main role in dissipating the input energy instead of the diagonal braces in prevalent braced frames. The seismic behavior of a type of braced frames with knee elements called Knee-Braced Frames (KBF) was also investigated by Balendra et al. [9]. In those frames,

* Corresponding author.

E-mail address: mass3001@yahoo.com (M. Mofid).

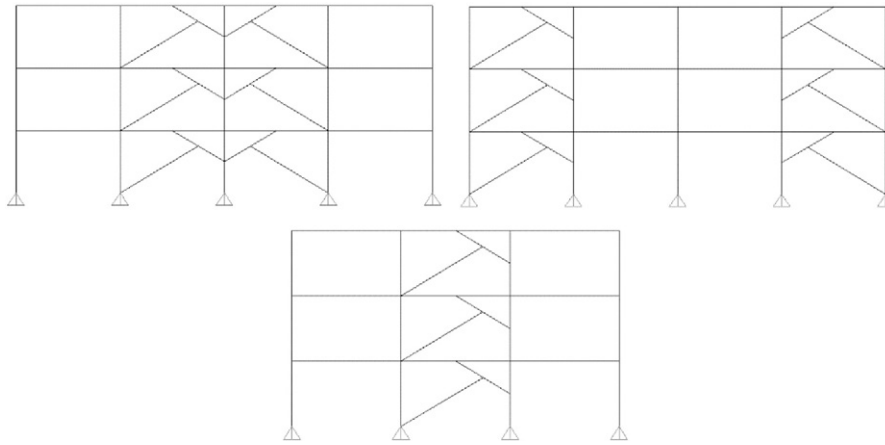


Fig. 1. The position of bracing members in 3 and 4-spans DKB archetypes.

buckling-resistant diagonal bracing elements provided significant lateral stiffness. At the same time, flexural or shear yielding of knee elements resulted in the ductility of structures under extreme dynamic excitation [10–12]. Furthermore, it has been proved that the story drifts of the braced frames with knee elements is less than the story drifts of moment resisting frames [13–15].

Regardless of all the mentioned merits of the DKB frames, implementing this type of frames as a prevalent lateral load resisting system in engineering practice demands for more investigation on their seismic performance. In this study, it has been attempted to investigate the behavior of 3, 5, 7 and 9-stories steel DKB frames. The initial objective of the investigation was to determine seismic performance factors of this type of braced frames. These factors would be required if a DKB frame is intended to be designed as a lateral load resisting system according to common design guidelines [16,17]. Numerous nonlinear static (push-over) analyses as well as incremental dynamic analyses (IDA) were conducted on archetype DKB frames as a part of this investigation. The numerical simulations have been performed using OpenSees simulation platform [18]. According to the results of the mentioned analyses and based on the procedure suggested by FEMA P695 [19], the required seismic performance factors for DKB frames were finally evaluated. The assessed seismic performance factors in this study includes the response modification factor (R), the over strength factor (Ω) and deflection amplification factor (C_d).

2. Development of archetype frames

In this research, several DKB frames were considered as the archetype frames. The set of archetypes involved frames with 3, 5, 7 and 9 stories were selected in order to consider the effect of the height of DKB

frames on their seismic response and seismic performance factors. Also in order to take into account different possible geometries for these frames, two types of frames with 3 and 4 spans were chosen. In 3-spans archetype frames, bracing members were located at the middle span while the bracing members were placed in the side spans in the archetypes with 4 spans as it has been shown in Fig. 1.

There is a significant difference between the ratios of seismic mass to gravity mass for peripheral and space frames. In order to take into account the effect of the mentioned difference, two sets of frames were chosen as the archetype frames in this study: a) space frames b) peripheral frames. The plan of the buildings consisting of these two types of archetype frames has been depicted in Fig. 2. All the frames of the first plan contribute in tolerating the lateral loading (space frames), whereas the lateral loading is carried out by only the first and the last frame (peripheral frames) in the second plan. It should be noted that, in the second plan with peripheral frames, the connections of central frames are all hinged.

Dead load and live load were considered equal to 5.5 kN/m^2 and 2 kN/m^2 respectively in order to design the frames. Length of all the beams was assumed to be equal to 3 m, while all the columns were assumed to be 5 m long. In order to include the seismic loading in the design procedure, the static lateral equivalent load was calculated for all the archetype frames based on the formulation proposed in section 12.8 of ACSE/SEI 07-10 [16]. On the other hand, several seismic design categories (SDC) were defined in this code named from SDC A to SDC E for the lowest to the highest probable seismic risk respectively. Intended DKB frames in this investigation can be used in seismic design categories B, C and D. Hence, the mentioned lateral equivalent force was conservatively calculated using the maximum design earthquake spectra suggested in FEMA P695 (Table 5-1) for Seismic Design Category D (SDC-D) [19]. Seismic performance factors required to calculate the lateral equivalent force

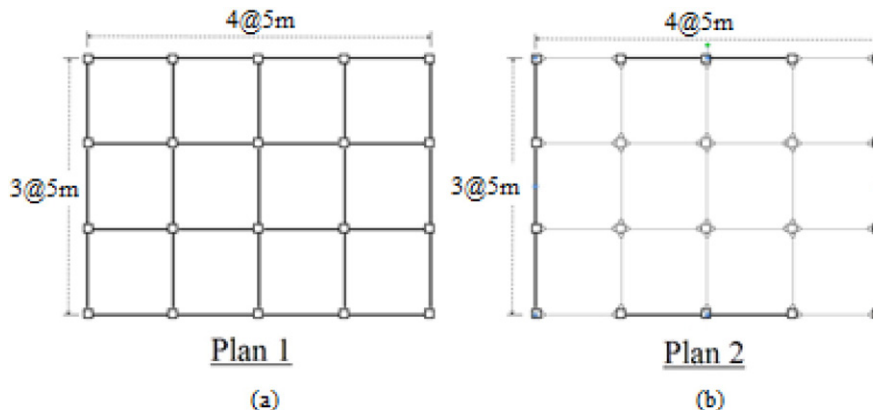


Fig. 2. Plan of the buildings consisting of (a) space frames; (b) peripheral frames.

Table 1
Summary of the design results for 4-span frames.

Story	Exterior columns	Interior columns	Bracing elements	Knee elements	Beams over bracings	Other beams
3-Story, 4-span, space frame (3S4b,S)						
1	IPB 260	IPB 260	Box 120 × 120 × 22.2	Box 120 × 120 × 22.2	IPB 260	IPB 260
2	IPB 260	IPB 260	Box 80 × 80 × 14.2	Box 80 × 80 × 14.2	IPB 260	IPB 260
3	IPB 260	IPB 260	Box 80 × 80 × 12.5	Box 80 × 80 × 12.5	IPB 240	IPB 240
5-Story, 4-span, space frame (5S4b,S)						
1,2	IPB300	IPB320	Box 120 × 120 × 22.2	Box 120 × 120 × 22.2	IPB 260	IPB 260
3,4	IPB240	IPB260	Box 100 × 100 × 17.5	Box 100 × 100 × 17.5	IPB 260	IPB240
5	IPB240	IPB240	Box 80 × 80 × 14.2	Box 80 × 80 × 14.2	IPB240	IPB240
7-Story, 4-span, space frame (7S4b,S)						
1	IPB300	IPB400	Box 140 × 140 × 22.2	Box 140 × 140 × 22.2	IPB280	IPB280
2,3	IPB300	IPB400	Box 100 × 100 × 17.5	Box 100 × 100 × 17.5	IPB280	IPB280
4	IPB240	IPB280	Box 100 × 100 × 17.5	Box 100 × 100 × 17.5	IPB240	IPB240
5,6,7	IPB240	IPB280	Box 80 × 80 × 14.2	Box 80 × 80 × 14.2	IPB240	IPB240
9-Story, 4-span, space frame (9S4b,S)						
1	IPB300	IPB500	Box 140 × 140 × 22.2	Box 140 × 140 × 22.2	IPB300	IPB300
2,3	IPB300	IPB400	Box 100 × 100 × 17.5	Box 100 × 100 × 17.5	IPB300	IPB260
4,5,6	IPB240	IPB300	Box 100 × 100 × 17.5	Box 100 × 100 × 17.5	IPB260	IPB240
7,8,9	IPB240	IPB280	Box 100 × 100 × 12.5	Box 100 × 100 × 12.5	IPB240	IPB240
3-Story, 4-span, peripheral frame (3S4b,P)						
1	IPB260	IPB300	Box 100 × 100 × 12.5	Box 140 × 140 × 22.2	IPB260	IPB260
2,3	IPB260	IPB260	Box 100 × 100 × 12.5	Box 120 × 120 × 22.2	IPB260	IPB240
5-Story, 4-span, peripheral frame (5S4b,P)						
1	IPB300	IPB360	Box 100 × 100 × 12.5	Box 160 × 160 × 22.2	IPB300	IPB260
2,3	IPB260	IPB300	Box 100 × 100 × 12.5	Box 160 × 160 × 22.2	IPB260	IPB260
4,5	IPB240	IPB260	Box 100 × 100 × 12.5	Box 140 × 140 × 12.2	IPB240	IPB240
7-Story, 4-span, peripheral frame (7S4b,P)						
1	IPB360	IPB500	Box 100 × 100 × 12.5	Box 160 × 160 × 22.2	IPB360	IPB260
2,3	IPB300	IPB450	Box 100 × 100 × 12.5	Box 160 × 160 × 22.2	IPB360	IPB260
4,5	IPB260	IPB360	Box 100 × 100 × 12.5	Box 140 × 140 × 17.5	IPB300	IPB240
6,7	IPB240	IPB280	Box 100 × 100 × 12.5	Box 140 × 140 × 17.5	IPB260	IPB240
9-Story, 4-span, peripheral frame (9S4b,P)						
1,2,3	IPB450	IPB700	Box 120 × 120 × 22.2	Box 200 × 200 × 22.2	IPB400	IPB400
4,5	IPB360	IPB400	Box 120 × 120 × 22.2	Box 160 × 160 × 22.2	IPB340	IPB340
6,7	IPB300	IPB400	Box 100 × 100 × 12.5	Box 160 × 160 × 17.5	IPB300	IPB300
8,9	IPB280	IPB300	Box 100 × 100 × 12.5	Box 160 × 160 × 17.5	IPB280	IPB280

were assumed at the first step. As an instance, the response modification factor was assumed to be equal to 8 according to the value suggested in Table 12-2-1 of ACSE/SEI 07-10 for eccentric brace frame [16]. The design procedure was then conducted based on the design criteria suggested by AISC 360-10 [17]. In addition, the relevant seismic provisions proposed by AISC 341-10 have been employed [20].

The yielding mode of link elements was considered to be of shear type during the design procedure. The yielding mode of these elements can be determined based on their length [9,12,20,21]. That is, the mode of yielding changes from flexural to shear by decreasing the length of knee element. In order to assure that the knee members have a shear-yielding mode instead of a flexural one, the maximum length of link elements (L_L) was limited as follow [21,22]:

$$L_L < 2M_p^*/V_p \quad (1)$$

where, M_p^* is the reduced plastic moment contributed by only flanges of the knee sections and V_p is the plastic shear force.

$$M_p^* = t_f \cdot b \cdot (d - t_f) \cdot \sigma_y \quad (2)$$

$$V_p = t_w \cdot (d - 2t_f) \cdot \frac{\sigma_y}{\sqrt{3}} \quad (3)$$

in which, σ_y , d , t_f , b , and t_w are the yielding stress, the depth, the flange thickness, the flange width and the web thickness of the knee elements respectively.

It is worthy to mention that the designed sections for the members of the peripheral frames were generally obtained larger compared with the sections assigned to the members of space frames. It can be simply justified considering the fact that the larger lateral loading should be tolerated by the peripheral frames than what is carried out

by space frames. The section of beam and column members were chosen among the standard IPB sections, while box sections utilized for braces and link elements were chosen during the design procedure. Furthermore, it was assumed that all the sections were fabricated from standard steel of type St37 with a yield strength equal to 240 MPa. For simplification, it was attempted to unify sections in the stories. Hence, the design results might be conservative for the members in some stories. A part of the design procedure results have been summarized in Table 1.

3. Scope and general frame work

The methodology introduced in FEMA P695 was implemented in this research to evaluate the seismic performance factors for the buildings that take advantage of DKB frames as their lateral load resisting system [19]. The methodology involves different steps from gathering

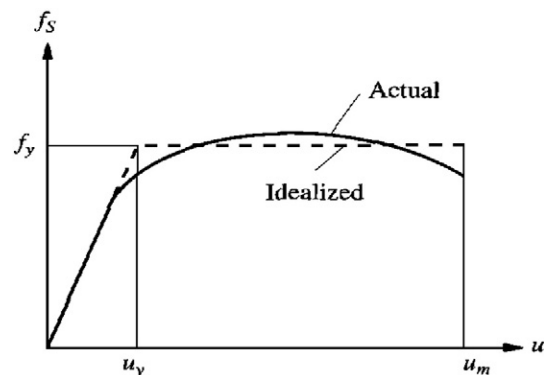


Fig. 3. General force-deformation curve beside an idealized bilinear curve.

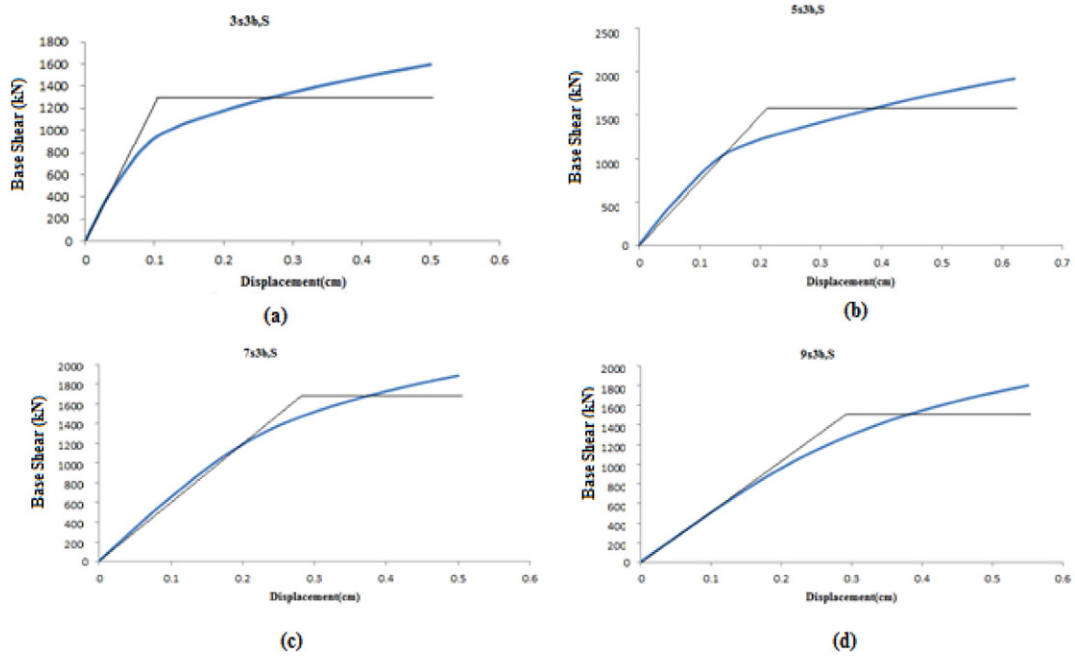


Fig 4. Pushover curves for the 3-bays space frame models with different number of stories.

information about the intended lateral load resisting system and selecting representative archetype frames all the way to conducting both nonlinear static and dynamic analyses. The uncertainties that might be involved following the steps of the methodology are implicitly considered as a part of this methodology. The uncertainties can be sourced from the uncertainties existing among different ground excitations and even they can be resulted because of the uncertainty of the modeling techniques used to simulate the behavior of different members. All in all, the implemented methodology is consisting three major steps as follow:

- Characterizing system behavior, and accordingly selecting numbers of representative index archetypes;

- Performing nonlinear static and dynamic analyses on the nonlinear models of the archetype frames.
- Assessing seismic performance factors based on the results of the analyses along with considering uncertainties involved in each step.

4. Defining performance groups

As it was stated before, numerous archetype frames were selected and designed in order to cover the different probable structural and geometric properties that can be expected for different general DKB frames. Archetypes DKB frames with different number of stories,

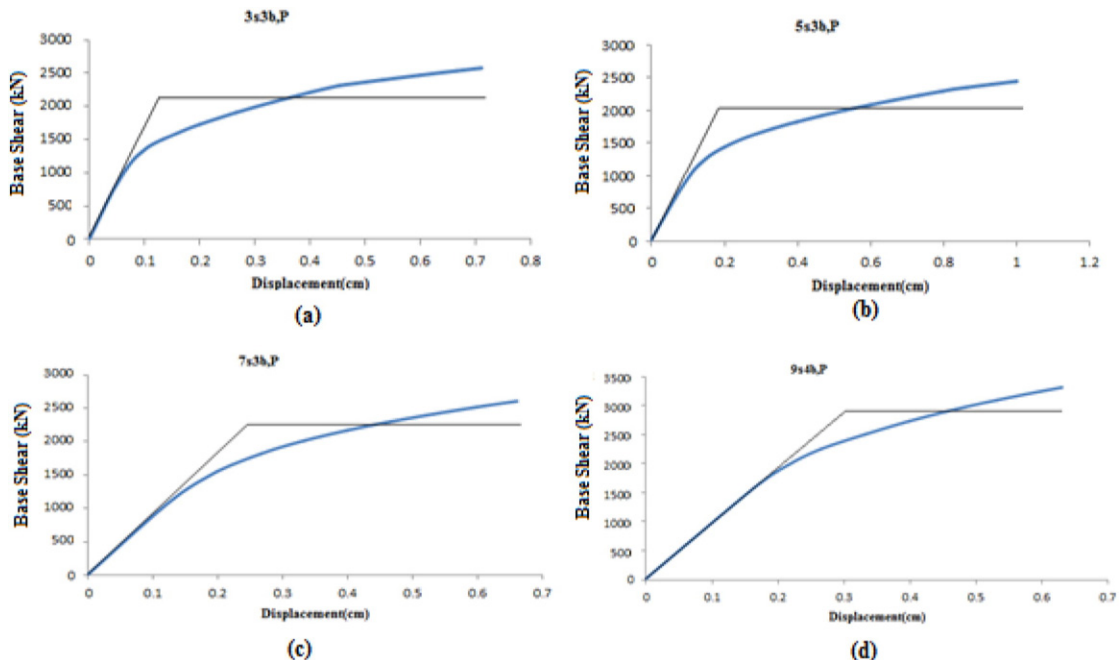


Fig 5. Pushover curves for the 3-bays peripheral frame models with different number of stories.

Table 2
Performance groups used in this research to categorize the archetype DKB frames.

Archetype name	Ratio of seismic mass to gravity mass
PG1	
3s2b,S	1
5s2b,S	1
7s2b,S	1
9s2b,S	1
PG2	
3s3b,P	2
5s3b,P	2
7s3b,P	2
9s3b,P	2
PG3	
3s4bm,S	1
5s4bm,S	1
7s4bm,S	1
9s4bm,S	1
PG4	
3s4bm,P	3
5s4bm,P	3
7s4bm,P	3
9s4bm,P	3
PG5	
3s3b,S	1
5s3b,S	1
7s3b,S	1
9s3b,S	1
PG6	
3s4bs,S	1
5s4bs,S	1
7s4bs,S	1
9s4bs,S	1
PG7	
5s4bs,P	3
7s4bs,P	3
9s4bs,P	3

different number of spans, different bracing arrangements and different seismic mass to gravity mass ratios were designed in this study. These archetype frames were then categorized to different performance groups. The archetypes in each group shared a common property. The performance groups defined in this paper and the archetype frames in each group have been summarized in Table 1. PG represents the term “Performance Group” in this table.

5. Numerical nonlinear analyses

In the methodology suggested by FEMA P695, collapse evaluation and establishing the seismic performance factors for a lateral load resisting system requires both nonlinear static and nonlinear dynamic analyses to be conducted on the nonlinear models of the archetype frames. Hence, numerical nonlinear models were provided for all the introduced archetype DKB frames as the first step to conduct required numerical simulations. Nonlinear modeling features of the OpenSees software [18] were utilized to develop the numerical models.

Columns were modeled with nonlinear beam-column elements while the cross-section of them was discretized to nonlinear fiber sections. Nonlinear behavior of beam members was considered through assigning nonlinear sections to the nonlinear beam-column elements. The section of beams was consisting of an Elastic Uniaxial Material in order to consider axial stiffness and a nonlinear Material with 2% hardening to consider flexural nonlinear behavior in these members. Concentrated plasticity model was used to simulate the nonlinear behavior of the Knee elements. Thus, these elements were composed of elastic beam-column elements as well as two zero-length elements at the ends of these elements. The zero length elements at the intersection of knee elements with beams and

columns represent flexural and shear nonlinear behavior of knee members. Nonlinear beam-column elements with fiber-based sections were employed in order to model bracing elements. In addition, an imperfection equal to 0.5% of the length of each brace was implemented in the middle of each member length to trigger buckling in these members [12,23]. This modeling technique makes it possible to capture the post buckling behavior of these elements.

5.1. Non-linear static (push-over) analyses

Nonlinear static analyses were performed using OpenSees simulation platform [18]. The lateral displacement loading and the analyses were aborted in case the rotation of the link elements exceeded 0.08 Rad. A triangular lateral load pattern along the height of the DKB frames is assumed. The amount of maximum base shear capacity V_{max} and ultimate displacement δ_u should be determined from the push-over analyses. Thus, V_{max} was considered as the maximum base shear regarding to the ultimate roof drift ratio. The estimated V_{max} and δ_u push-over analyses results were then utilized to evaluate the over strength factor, Ω , as well as, the period-based ductility, μ_T , for each archetype frame. The over strength factor for all models was determined as the ratio of the maximum base shear capacity to the design base shear.

$$\Omega = \frac{V_{max}}{V} \quad (4)$$

On the other hand, the period-base ductility μ_T was calculated as the ratio of ultimate roof displacement δ_u to the effective yield roof displacement.

$$\mu_T = \frac{\delta_u}{\delta_{y,eff}} \quad (5)$$

where, the effective yield roof displacement was defined as follow:

$$\delta_{y,eff} = C_0 \frac{V_{max}}{W} \left[\frac{g}{4\Gamma^2} \right] \left((\max(T, T_1))^2 \right) \quad (6)$$

The coefficient C_0 relates the SDOF displacement to the roof displacement of MDOF [19], W is building weight, g is the gravity constant, T is the fundamental period and T_1 is the fundamental period of each model obtained from an eigenvalue analysis. The coefficient C_0 according to is given by the following formula:

$$C_0 = \phi_{1,r} \frac{\sum_1^N m_x \phi_{1,x}}{\sum_1^N m_x \phi_{1,x}^2} \quad (7)$$

where, $\phi_{1,x}$ ($\phi_{1,r}$) is the ordinate of the fundamental mode at level x (roof), and N is the number of levels [19].

5.1.1. Elastoplastic idealizations

The push-over curves obtained from the numerical analyses were also idealized to simple bilinear curves as it is schematically shown in Fig. 3. The idealized bilinear curves were drawn in a way that the area under these curves was obtained equal to the area under the original curves derived from the analyses. Fig. 4 and Fig. 5 illustrate the idealized push-over curve as well as the curves obtained from the simulations for the 3, 5, 7 and 9-stories DKB frames. Furthermore, the results of the nonlinear static (push-over) analyses are summarized in Table 2 and Table 3 for the space and peripheral DKB archetype frames, respectively.

As it is apparent from Table 3 and Table 4, large values were obtained for the over strength factor of the 3 and 5-stories space frames. It should be also noted that the value of the over strength factor decreased considerably by increasing the height of the archetype frames. As it is expected, this seismic performance factor was obtained larger for the peripheral frames compared to the values calculated for the space frames. The

Table 3
Summary of nonlinear static analyses for the space archetype frames.

Model ID	Period(sec)	δy_{eff}	δu	V max(kN)	μ	Ω
3s2b,S	0.45	0.032	0.254	870	7.9	3.9
3s3b,S	0.51	0.039	0.5	1300.5	12.5	3.92
3s4bm,S	0.51	0.036	0.55	1609.8	15.2	3.64
3s4bs,S	0.51	0.03	0.22	1354	7.2	3.06
5s2b,S	0.73	0.059	0.4	1125	6.6	3.05
5s3b,S	0.78	0.064	0.62	1601	9.7	2.89
5s4bm,S	0.727	0.061	0.85	2307.2	13.9	3.13
5s4bs,S	0.737	0.065	0.71	2401	10.9	3.26
7s2b,S	0.994	0.088	0.51	1305	5.7	2.53
7s3b,S	1.035	0.076	0.5	1580	6.5	2.04
7s4bm,S	0.926	0.065	0.6	2253	9.1	2.18
7s4bs,S	0.99	0.08	0.55	2383	6.8	2.31
9s2b,S	1.287	0.109	0.71	1283.5	6.4	1.93
9s3b,S	1.333	0.091	0.55	1502.3	6	1.51
9s4bm,S	1	0.097	0.65	1870	7.5	1.41
9s4bs,S	1.213	0.098	0.67	2603	6.8	1.96

reason for that is the fact that the peripheral frames were designed based on more severe loading.

5.2. Nonlinear dynamic analysis

As it was mentioned, a presumed response modification factor, R, was utilized to design the archetype frames. In this step, the seismic performance of the designed frames should be assessed through conducting numerous nonlinear incremental dynamic analyses (IDA) under several ground motion records. If the seismic performance of the archetype frames could not be accepted, a new value for R should be considered and the procedures should be repeated. In order to perform the assessment, the collapse capacity of the archetype frames should be quantified implementing an index proposed by FEMA P695 and named collapse margin ratio (CMR). The acceptance margin for the indexes evaluated for different frames are also provided in that report. Nonlinear dynamic analyses were applied to evaluate the median collapse capacity, S_{CT} as well as the CMR for each archetype model.

Earthquake records suggested by FEMA P695 were chosen in order to perform the required IDAs [19]. Two sets of ground-motion records were collected for this purpose in the mentioned report. The first set contains 22 ground motion far field record pairs, while the second set includes 28 pairs of near field earthquake records. Both records of each pair were recorded at the same point but in perpendicular directions. In this study, the far field record set that is consisting of 44 individual records was employed to conduct the numerical analyses. The collapse limit state for each archetype frame was considered as the time in which the maximum story-drift ratio exceeds 10% according to Vamvatsikos and Cornell [24].

The chosen earthquake records had been scaled in two steps before they were employed to run the IDAs. At the first step, the records were normalized by their peak ground velocity in the purpose that the unwarranted variability between records should be omitted. However, it should be noted that the frequency content of the seismic records was not affected by this scaling procedure. As the second step, the records normalized in the previous step were collectively anchored to a specific ground motion intensity. That is, the median spectral acceleration of all the record in the set fitted to the design spectral acceleration at the fundamental period of each intended archetype model before conducting the IDAs. In order to perform the IDAs, each archetype model was subjected to each of 44 individual records with increasing intensity. After performing 44 time-history analyses under all the 44 records with a specific intensity level, the intensity of the set of records was then scaled up to conduct another 44 time-history analyses under the records with the new intensity level. A summary of the results obtained from the nonlinear incremental dynamic analyses has been presented in Table 5 and Table 6.

5.3. Determination of median collapse capacity

After conducting the incremental dynamic analyses, median collapse capacity and the CMR can be evaluated for all the archetype frames based on the analyses results. Median collapse capacity, S_{CT} , is defined as the ground motion intensity level in which half of the implemented records cause collapse of an archetype model [19]. On the other hand, the ratio of the median collapse intensity to the MCE intensity for each frame is defined as the collapse margin ratio (CMR) of that frame. MCE intensity (S_{MT}) was obtained from the MCE design spectrum suggested by FEMA P695 for the seismic design category D_{max} at the fundamental period of each archetype model.

$$CMR = \frac{S_{CT}}{S_{MT}} \quad (8)$$

Collapse margin ratio indicates the safety margin for an intended structure. Fig. 6 shows the incremental dynamic analyses results for

Table 4
Summary of nonlinear static analyses for the peripheral archetype frames.

Model ID	Period(sec)	δy_{eff}	δu	V max(kN)	μ	Ω
3s3b,P	0.5	0.049	0.71	2124	14.36	5.19
3s4bm,P	0.555	0.041	0.75	2304	18.07	3.55
3s4bs,P	0.538	0.039	0.36	2237	9.15	3.45
5s3b,P	0.826	0.071	1	2000	14.01	2.93
5s4bm,P	0.794	0.067	1.2	3253.5	17.88	3.01
5s4bs,P	0.817	0.073	1	3337	13.53	3.08
7s3b,P	1.014	0.083	0.66	2243.5	7.94	2.35
7s4bm,P	0.988	0.071	0.6	3255	8.35	2.15
7s4bs,P	1.006	0.079	0.51	3402.7	6.39	2.25
9s3b,P	1.062	0.091	0.63	2900.5	6.95	2.36
9s4bm,P	0.979	0.083	0.8	4975.3	9.6	2.56
9s4bs,P	1.081	0.082	0.5	4005.5	6.02	2.06

the 3 and 5 stories space and peripheral archetype frames. The CMR values calculated for different archetype frames have been listed in Table 5 and Table 6.

5.3.1. Adjusted collapse margin ratio (ACMR)

To consider unique attributes of severe ground excitations which can cause detrimental effect on the seismic response of a structure, the collapse margin ratio is rectified to an adjusted collapse margin ratio. This adjustment was performed using a factor called Spectral Shape Factor (SSF) in order to consider the effects of the spectral shape of the records which were used to assess CMR value [19].

$$ACMR_i = SSF_i \cdot CMR_i \quad (9)$$

Spectral Shape Factor (SSF) can be evaluated as a function of the fundamental period, T , and the period-based ductility, μ_T , of a frame as well as the seismic design category of interest. Spectral shape factors employed in this study were extracted from Table 7-1 of FEMA P695 [19]. In that table, the structures with higher ductility and longer periods merit larger adjustments.

6. Considering the effect of inevitable uncertainties in the study

Different types of uncertainties that might affect the obtained results were also considered implicitly to make the final decision about the seismic performance factor as reliable as possible. First, all significant uncertainty sources were recognized. The sources of uncertainty can be enumerated as follow: Record To Record (RTR) uncertainty, design requirement (DR) uncertainty, Modeling uncertainty (MDL), and test data (TD) uncertainty. Record To Record uncertainty can be interpreted as the variability in the response of a numerical model under various ground motions. The uncertainty might be involved in the design

Table 5
Summary of nonlinear dynamic analysis for peripheral frames.

Model	S_{CT}	S_{MT}	CMR	SSF	ACMR
3 stories					
3s3b,P	3.55	1.5	2.37	1.33	3.15
3s4bm,P	3.86	1.5	2.57	1.34	3.44
3s4bs,P	3.74	1.5	2.49	1.34	3.34
5 Stories					
5s3b,P	3.72	1.4	2.66	1.42	3.78
5s4bm,P	4.02	1.4	2.87	1.41	4.05
5s4bs,P	3.95	1.4	2.82	1.42	4
7 stories					
7s3b,P	2.12	0.92	2.3	1.46	3.36
7s4bm,P	2.24	0.92	2.43	1.46	3.55
7s4bs,P	2.21	0.92	2.4	1.46	3.5
9 stories					
9s3b,P	1.31	0.85	1.54	1.46	2.25
9s4bm,P	1.52	0.85	1.79	1.46	2.61
9s4bs,P	1.48	0.85	1.74	1.46	2.54

criteria implemented in order to design the archetypes frames that is represented by design requirement uncertainty. The probable inaccuracy in the numerical modeling procedure is represented by modeling uncertainties. Furthermore, test data uncertainties are relevant to the quality of the test data used to calibrate the numerical modeling techniques used in this study.

Different lognormal standard deviation parameters (β) can be defined to represent the effect of each of the aforementioned uncertainties. These parameters are evaluated according to separated tables provided by FEMA P695 [19]. The tables illustrated four levels of uncertainty distinguished with the terms of superior, good, fair and poor with lognormal standard deviation parameters equal to 0.1, 0.2, 0.35 and 0.5 respectively. In this research, the values of lognormal standard deviation parameters for different mentioned uncertainties, β_{RTR} , β_{DR} , β_{MDL} and β_{TD} , were selected equal to 0.4, 0.1, 0.2 and 0.35 respectively.

6.1. Total collapse uncertainty

The total collapse uncertainty should be estimated by applying all types of uncertainty that were mentioned above. Hence, the collapse fragility of each archetype model can be represented by a random variable, S_{CT} , defined as follow:

$$S_{CT} = S_{CT} \lambda_{TOT} \quad (10)$$

where S_{CT} can be obtained from the IDAs, and λ_{TOT} is presumed as the random variable with log-normal distribution as well as a median value of unity and a standard deviation of β_{TOT} . On the other hand, the random variable λ_{TOT} can be defined as:

$$\lambda_{TOT} = \lambda_{RTR} \lambda_{DR} \lambda_{TD} \lambda_{MDL} \quad (11)$$

In this formula, λ_{RTR} , λ_{DR} , λ_{TD} , and λ_{MDL} are again assumed to have a median value of unity and lognormal distribution with standard deviation parameters, β_{RTR} , β_{DR} , β_{MDL} and β_{TD} respectively. In addition, four mentioned random variables are supposed to be statically independent. Thus, β_{TOT} , as the standard deviation parameter which represent the total collapse uncertainty, can be given by:

$$\beta_{TOT} = \sqrt{\beta_{RTR}^2 + \beta_{DR}^2 + \beta_{TD}^2 + \beta_{MDL}^2} \quad (12)$$

Eventually, the total lognormal standard deviation parameter, β_{TOT} , was calculated equal to 0.577 in this investigation.

6.2. Collapse fragility curve

The collapse fragility curve can be drawn as a Cumulative Distribution Function (CDF) which relates the ground motion excitation intensity to a certain probability of collapse. Such a curve can be derived from the outcome of incremental dynamic analyses. Two collapse fragility curves have been depicted in Fig. 7. The dashed fragility curve was

Table 6
Summary of nonlinear dynamic analysis for space frames.

Model	S_{CT}	S_{MT}	CMR	SSF	ACMR
3 stories					
3s2b,S	3.52	1.5	2.35	1.33	3.13
3s3b,S	3.35	1.5	2.23	1.33	2.97
3s4bm,S	3.76	1.5	2.51	1.33	3.34
3s4bs,S	3.43	1.5	2.29	1.33	3.05
5 stories					
5s2b,S	3.64	1.4	2.6	1.38	3.59
5s3b,S	3.77	1.4	2.69	1.39	3.74
5s4bm,S	3.95	1.4	2.82	1.38	3.89
5s4bs,S	3.89	1.4	2.78	1.38	3.84
7 stories					
7s2b,S	2.12	0.92	2.3	1.46	3.36
7s3b,S	2.26	0.92	2.46	1.46	3.59
7s4bm,S	2.32	0.92	2.52	1.45	3.65
7s4bs,S	2.35	0.92	2.55	1.46	3.72
9 stories					
9s2b,S	1.42	0.92	1.54	1.54	2.37
9s3b,S	1.12	0.92	1.22	1.55	1.89
9s4bm,S	1.53	0.92	1.66	1.51	2.51
9s4bs,S	1.24	0.92	1.35	1.52	2.05

drawn considering only RTR uncertainty. However, the solid curve represents a fragility curve when a standard deviation parameter, β_{TOT} , equal to 0.577 was taken into account. Therefore, as shown in Fig. 7, considering uncertainties can decrease the slope of a fragility curve. In other words, the collapse probability for the seismic intensities less than the median collapse capacity increased when all the mentioned uncertainties were taken into account.

7. Evaluation of seismic performance factor

7.1. Evaluation of response modification coefficient

Accepting the presumed value for the response modification factor is according to two principle criteria:

- The average adjusted collapse margin ratio for each performance group must be greater than the acceptable adjusted collapse margin ratio accepting 10% collapse probability.

$$\overline{ACMR}_i \geq ACMR_{10\%}$$

- The value of adjusted collapse margin ratio for each model must be greater than adjusted collapse margin ratio with 20% collapse probability.

$$ACMR_i \geq ACMR_{20\%}$$

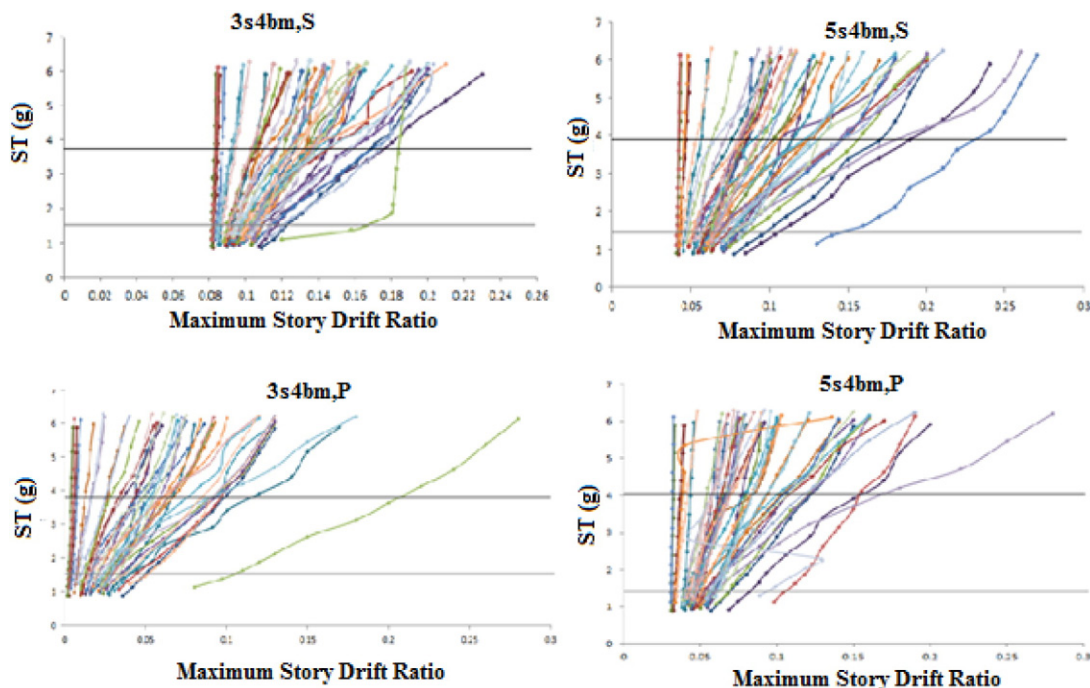


Fig. 6. IDA curves of the 3 and 5-stories space and peripheral archetype frames with 4 bays.

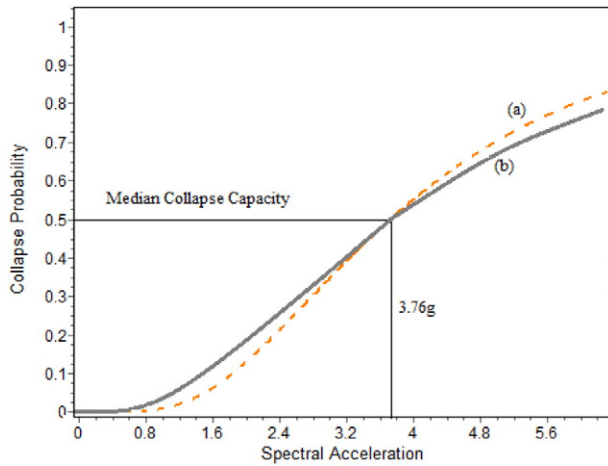


Fig. 7. Collapse fragility curves (a) considering only Record To Record uncertainty, (b) considering all the uncertainties.

According to Table 7 and the acceptable ACMRs provided in Table 7-3 of FEMA P695 [19], both the criteria were met for all the performance groups as well as all the archetype frames. Therefore, it can be concluded that the presumed response modification factor for disposable knee bracing system ($R = 8$) can be established for these lateral load resisting systems.

7.2. Evaluation of over-strength factor

The acceptable value of over-strength factor should not be less than the maximum of average over-strength values determined for the performance groups. Moreover, this factor must be conservatively rounded to half unit intervals [19]. The system over-strength factor should be also less than 1.5 times the response modification factor. On the other hand, the value of this factor should be restricted to 3 as described in Table 12.2-1 of ASCE/SEI 7-10 [16]. Thus, as indicated by Table 7, the maximum average value of over-strength factor was obtained equal to 3.25 in this research, which can be rounded to 3.5. However, this factor was suggested to be equal to 3 based on the mentioned limitation.

7.3. Evaluation of deflection amplification factor

The deflection amplification factor was estimated based on the accepted value for the response modification factor as follow:

$$C_d = \frac{R}{B_1} \quad (13)$$

where B_1 is the damping coefficient that can be evaluated referring to Table 18.6-1 ASCE/SEI 7-10 [16]. If the inherent damping is assumed to be equal to 5%, this coefficient is equal to 1. Hence, the value of the deflection amplification factor is chosen equal to the value of response modification factor for buildings with DKB frames.

8. Summary and conclusions

In this study, a theoretical investigation was conducted in order to assess the behavior of 3, 5, 7 and 9-stories disposable knee bracing steel frames. First, the nonlinear static analyses were conducted to provide statistical data on over-strength and period-based ductility of the intended archetype frames. Henceforth, a simple collapse assessment was performed using nonlinear incremental dynamic analyses. Finally, the acceptability of presumed seismic performance factors was checked

Table 7
Establishing seismic performance factors.

Model ID	Ω	ACMR	$\overline{ACMR} \geq ACMR_{10\%} = 2.12$	$ACMR \geq ACMR_{20\%} = 1.64$
PG1				
3s2b,S	3.9	3.13	Checked	Checked
5s2b,S	3.05	3.59	Checked	Checked
7s2b,S	2.53	3.36	Checked	Checked
9s2b,S	1.93	2.37	Checked	Checked
\overline{ACMR}		3.112		
$\overline{\Omega}$	2.85			
PG2				
3s3b,P	5.19	3.15	Checked	Checked
5s3b,P	2.93	3.78	Checked	Checked
7s3b,P	2.53	3.36	Checked	Checked
9s3b,P	2.36	2.25	Checked	Checked
\overline{ACMR}		3.135		
$\overline{\Omega}$	3.25			
PG3				
3s4bm,S	3.64	3.34	Checked	Checked
5s4bm,S	3.13	3.89	Checked	Checked
7s4bm,S	2.18	3.65	Checked	Checked
9s4bm,S	1.41	2.51	Checked	Checked
\overline{ACMR}		3.347		
$\overline{\Omega}$	2.59			
PG4				
3s4bm,P	3.55	3.44	Checked	Checked
5s4bm,P	3.01	4.05	Checked	Checked
7s4bm,P	2.15	3.55	Checked	Checked
9s4bm,P	2.56	2.61	Checked	Checked
\overline{ACMR}		3.4125		
$\overline{\Omega}$	2.82			
PG5				
3s3b,S	3.92	2.97	Checked	Checked
5s3b,S	2.89	3.74	Checked	Checked
7s3b,S	2.04	3.59	Checked	Checked
9s3b,S	1.51	1.89	Checked	Checked
\overline{ACMR}		3.0475		
$\overline{\Omega}$	2.59			
PG6				
3s4bs,S	3.06	3.05	Checked	Checked
5s4bs,S	3.26	3.84	Checked	Checked
7s4bs,S	2.31	3.72	Checked	Checked
9s4bs,S	1.96	2.05	Checked	Checked
\overline{ACMR}		3.165		
$\overline{\Omega}$	2.65			
PG7				
3s4bs,P	3.45	3.34	Checked	Checked
5s4bs,P	3.08	4	Checked	Checked
7s4bs,P	2.25	3.5	Checked	Checked
9s4bs,P	2.06	2.54	Checked	Checked
\overline{ACMR}		3.345		
$\overline{\Omega}$	2.71			

based on the seismic performance of the archetype frames. The following conclusions can be made from the results:

- 1) The results of nonlinear static analyses (push-over) indicated that the efficiency of link elements to improve the ductility of structures decreased by increasing the number of stories. As an instance, in 3-stories space frames, the value of ductility factor was approximately 10. However, that value are reduced to approximately 6 for the 9-stories frames. It should be also noted that the above-mentioned values obtained greater for peripheral frames than those of space frames.
- 2) The results of incremental nonlinear static analyses revealed that the amount of over-strength factor was generally decreased in the space frames by increasing the number of stories. For instance, the over-strength factor took the value of 3.9 in case of the 3-stories frame

with 2 spans. However, the value of this factor reached to 1.93 by increasing the number of stories.

- 3) The results of non-linear dynamic analyses presented in this paper foregrounded the fact that by increasing the number of stories, the amount of collapse margin ratio reduced considerably in both space and peripheral frames.
- 4) According to the results of this study and also based on the criteria mentioned in FEMA P695, the value of response modification factor for the building with disposable knee bracing frames was proposed equal to 8. It was also concluded that the amount of deflection amplification factor, C_d , should be equal to the value of the response modification factor.
- 5) As an economical consideration, the application of link elements in steel frame structures is acceptable. Moreover, these elements can play a significant role in the rehabilitation and repair of existing buildings.

References

- [1] T. Balendra, E.L. Lim and S.L. Lee, "Ductile knee braced frames with shear yielding knee for seismic resistant structures", Butterworth-Heinemann, J. Struct. Eng., 1994, vol. 16, Number 4, pp. 263-269.
- [2] T. Balendra, M.T. Sam, C.Y. Uaw, "Diagonal brace with ductile knee anchor for aseismic steel frame", John Wiley & Sons, Earthq. Eng. Struct. Dyn. 19 (1990) 847–858.
- [3] E.P. Popov, "Recent research on eccentrically braced frames", Butterworth and Co., Struct. Eng., vol. 5, Jan. 1983. B
- [4] C.W. Roeder, E.P. Popov, Inelastic behavior of eccentrically braced steel frames under cyclic loadings, EERC Report 77-18, University of California, Berkeley, California, 1977.
- [5] C.W. Roeder, E.P. Popov, Eccentrically braced steel frames for earthquakes, J. Struct. Div. 104 (1978) 391–411 ASCE.
- [6] A. Ghobarah, H. Abou Elfath, "Rehabilitation of a reinforced concrete frame using eccentric steel Bracing", Elsevier, J. Eng. Struct. 23 (2001) 745–755.
- [7] H.W. Spurr, Wind Bracing, McGraw-Hill Book Co., New York, 1930.
- [8] D. Aristizabal-Ochoa, "Disposable knee bracing: improvement in seismic design of steel frames", J. Struct. Eng. 112 (1986) 1544–1552 ASCE.
- [9] T. Balendra, M.T. Sam, C.Y. Liaw, Design of earthquake-resistant steel frames with knee bracing", Elsevier, J. Constr. Steel Res. (1991) 193–207.
- [10] M. S. Williams, A. Blakeborough, D. Clément and N. Bourahla, "Seismic behavior of knee braced frames", Williams et al., Structures & Buildings, vol. 152, Issue 2, May 2002, pp. 147–155.
- [11] T. Okazaki, M.D. Engelhardt, "Cyclic loading behavior of EBF links constructed of ASTM A992 steel", Elsevier, J. Constr. Steel Res. 63 (2007) 751–765.
- [12] M. Farahi, M. Mofid, "On the quantification of seismic performance factors of Chevron knee bracings, in steel structures", Elsevier, Eng. Struct. 46 (2013) 155–164.
- [13] J.R. Libby, Eccentrically braced frame construction—a case history, Eng. J. (1981) AISC, 4th qtr.
- [14] E.P. Popov, M.D. Engelhardt, "Seismic Eccentrically Braced Frames", Elsevier, J. Constr. Steel Res. 10 (1988) 321–354.
- [15] D.N. Manheim, On the design of eccentrically braced frames, D. Eng. Thesis, Department of Civil Engineering, University of California, Berkeley, USA, February 1982.
- [16] ASCE/SEI 7-10, Minimum Design Loads for Buildings and Other Structures, American Society of Civil Engineering, 2010.
- [17] ANSI/AISC 360-10, Load and Resistance Factor Design Specification for Structural Steel Buildings, American Institute of Steel Construction, Inc., Chicago, IL, 2010.
- [18] Open System for Earthquake Engineering Simulation (OpenSees) Framework. Pacific Earthquake Engineering Research Center, University of California, Berkeley. <<http://opensees.berkeley.edu/>>.
- [19] FEMA, Quantification of building seismic performance factors, FEMA P695, Federal Emergency Management Agency, Washington, DC, June 2009.
- [20] ANSI/AISC 341-05, Seismic Provisions for Structural Steel Buildings, American Institute of Steel Construction, Inc., Chicago, IL, 2005.
- [21] M. Lotfollahi, M. Mofid, On the design of new ductile knee bracing, J. Constr. Steel Res. 62 (2006) 282–294.
- [22] M. Mofid, M. Lotfollahi, "On the characteristics of new ductile knee bracing systems", Elsevier, J. Constr. Steel Res. 62 (2006) 271–281.
- [23] P. Uriz, S.A. Mahin, Toward Earthquake-Resistant Design of Concentrically Braced Steel-Frame Structures, Pacific Earthquake Engineering Research Center, PEER2008-08, 2008.
- [24] D. Vamvatsikos, C.A. Cornell, Applied incremental dynamic analysis, Earthq. Eng. Struct. Dyn. 31 (3) (2002) 491–514.